Cellular/Molecular

Identification of a $GABA_A$ Receptor Anesthetic Binding Site at Subunit Interfaces by Photolabeling with an Etomidate Analog

Guo-Dong Li,[1]* David C. Chiara,[2]* Gregory W. Sawyer,[1] S. Shaukat Husain,[3] Richard W. Olsen,[1] and Jonathan B. Cohen[2]

[1]Department of Molecular and Medical Pharmacology, Geffen School of Medicine, University of California at Los Angeles, Los Angeles, California 90095, [2]Department of Neurobiology, Harvard Medical School, Boston, Massachusetts 02115, and [3]Department of Anesthesia and Critical Care, Massachusetts General Hospital, Boston, Massachusetts 02114

General anesthetics, including etomidate, act by binding to and enhancing the function of GABA type A receptors ($GABA_A$Rs), which mediate inhibitory neurotransmission in the brain. Here, we used a radiolabeled, photoreactive etomidate analog ([^{3}H]azietomidate), which retains anesthetic potency *in vivo* and enhances $GABA_A$R function *in vitro*, to identify directly, for the first time, amino acids that contribute to a $GABA_A$R anesthetic binding site. For $GABA_A$Rs purified by affinity chromatography from detergent extracts of bovine cortex, [^{3}H]azietomidate photoincorporation was increased by GABA and inhibited by etomidate in a concentration-dependent manner ($IC_{50} = 30\ \mu M$). Protein microsequencing of fragments isolated from proteolytic digests established photolabeling of two residues: one within the αM1 transmembrane helix at α1Met-236 (and/or the homologous methionines in α2,3,5), not previously implicated in etomidate function, and one within the βM3 transmembrane helix at β3Met-286 (and/or the homologous methionines in β1,2), an etomidate sensitivity determinant. The pharmacological specificity of labeling indicates that these methionines contribute to a single binding pocket for etomidate located in the transmembrane domain at the interface between β and α subunits, in what is predicted by structural models based on homology with the nicotinic acetylcholine receptor to be a water-filled pocket ~50 Å below the GABA binding site. The localization of the etomidate binding site to an intersubunit, not an intrasubunit, binding pocket is a novel conclusion that suggests more generally that the localization of drug binding sites to subunit interfaces may be a feature not only for GABA and benzodiazepines but also for etomidate and other intravenous and volatile anesthetics.

Key words: **$GABA_A$ receptor; anesthesia; structure; photolabeling; nicotinic receptor; muscimol; binding; etomidate**

Introduction

GABA type A receptors ($GABA_A$Rs) are the molecular targets for general anesthetic action in the brain. Anesthetics of diverse chemical structure, including inhalants, neuroactive steroids, and intravenous general anesthetics such as etomidate, propofol, and barbiturates, all enhance $GABA_A$R currents *in vitro* at doses consistent with their action as anesthetics *in vivo* (Olsen et al., 1986; Franks and Lieb, 1994; Yamakura et al., 2001; Hemmings et al., 2005).

The $GABA_A$R is a member of the Cys-loop superfamily of ligand-gated ion channels that also includes the nicotinic acetylcholine receptors (nAChRs), from which much of the general structure of this superfamily is inferred (Corringer et al., 2000; Sine and Engel, 2006). Each receptor is composed of a pentamer of homologous subunits arranged around a central axis. Each subunit transmembrane domain (TMD) is a bundle of four α helices (M1–4), with M2 from each subunit forming the wall of the ion channel. $GABA_A$R homology models can be constructed by using the structures of the soluble snail acetylcholine binding protein structure (Brejc et al., 2001) and the *Torpedo* nAChR (Miyazawa et al., 2003). The two transmitter binding sites are within the receptor extracellular domain at subunit interfaces (β–α for $GABA_A$R), and the benzodiazepine binding site is at the equivalent position at the α–γ interface (Cromer et al., 2002; Ernst et al., 2005).

Mutational analyses have identified positions in the $GABA_A$R TMD that are important for the GABA-enhancing effects of alcohols and volatile and intravenous anesthetics (Mihic et al., 1997; Olsen et al., 2004), with a binding pocket proposed for volatile anesthetics inside the helical bundle of a given subunit involving residues M2–15 and M3–4, numbered relative to the N-terminal charge of each helix (Mihic et al., 1997; Yamakura et al., 2001). The M2–15 residue also determines the selectivity of β

Received Aug. 10, 2006; revised Sept. 25, 2006; accepted Sept. 28, 2006.

This work was supported in part by United States Public Health Service Grant GM58448 (Keith Miller, R.W.O., J.B.C.) and by an award to the Harvard Medical School from the Howard Hughes Medical Institute Biomedical Research Support Program. We thank Keith Miller and Stu Forman for useful discussions during the course of this work.

*G.-D.L and D.C.C. contributed equally to this work.

Correspondence should be addressed to either of the following: Richard W. Olsen, Department of Molecular and Medical Pharmacology, Geffen School of Medicine, University of California at Los Angeles, Los Angeles, CA 90095, E-mail: rolsen@mednet.ucla.edu; or Jonathan B. Cohen, Department of Neurobiology, Harvard Medical School, Boston, MA 02115, E-mail: jonathan_cohen@hms.harvard.edu.

G. W. Sawyer's present address: Department of Biochemistry and Microbiology, Center for Health Sciences, Oklahoma State University, Tulsa, OK 74107.

DOI:10.1523/JNEUROSCI.3467-06.2006

 0270-6474/06/2611599-07$15.00/0

subunits for etomidate *in vitro* (Belelli et al., 1997), and a knock-in mouse for β3N265M shows reduced sensitivity to the anesthetic effects of etomidate and propofol (Jurd et al., 2003).

In the absence of structural information, it remains uncertain whether these positions contribute directly to an anesthetic binding site or are involved in allosteric modulation of gating. Photoaffinity labeling, which provides an experimental approach to directly identify amino acids contributing to a drug binding site without previous assumptions about the protein points of contact (Kotzyba-Hibert et al., 1995), has been used extensively to identify amino acids contributing to ligand binding sites in the *Torpedo* nAChR (Mourot et al., 2006) and for $GABA_AR$ agonists and benzodiazepines (Smith and Olsen, 1994; Duncalfe et al., 1996; Sawyer et al., 2002). We now use 2-(3-methyl-3*H*-diaziren-3-yl) ethyl 1-(1-phenylethyl)-1*H*-imidazole-5-carboxylate ([^{3}H]azietomidate), a photoreactive analog of etomidate that retains anesthetic and $GABA_AR$ modulatory properties (Husain et al., 2003), to provide the first identification of amino acids contributing to an anesthetic binding site in a $GABA_AR$. The two labeled residues, αM1–14 (αMet-236) and βM3–4 (βMet-286), are shown by homology modeling to border a pocket in the TMD located at the same subunit interfaces that contain the GABA binding site in the extracellular domain. The αM1 helix has not been implicated previously in etomidate function, whereas βM3–4 is an anesthetic sensitivity determinant (Mihic et al., 1997; Krasowski et al., 1998; Bali and Akabas, 2004). Furthermore, the homology model suggests that this intersubunit etomidate binding pocket is in contact with βM2–15, an *in vivo* etomidate anesthetic sensitivity determinant (Jurd et al., 2003).

Materials and Methods

Materials. [^{3}H]azietomidate (11 Ci/mmol) was synthesized as described previously (Husain et al., 2003). (Sources of antibodies and reagents are described in the supplemental Materials and Methods, available at www.jneurosci.org as supplemental material.)

Solubilization and purification of bovine brain $GABA_ARs$. $GABA_AR$ was purified by modification of previous protocols (Sigel and Barnard, 1984; Sawyer et al., 2002) on a benzodiazepine Ro7/1986-1 affinity column. Detailed conditions for solubilization and purification as well as the immunoblot and mass spectrometry protocols for characterization of the purified $GABA_AR$ are described in the supplemental Materials and Methods (available at www.jneurosci.org as supplemental material). Important modifications that allowed ~5000-fold purification of $GABA_AR$ at high yield and with retention of positive allosteric modulation of [^{3}H]muscimol binding by etomidate included: (1) the use of the detergent $C_{12}E_9$ in conjunction with 3-[(3-cholamidopropyl) dimethylammonio]-1-propanesulfonate (CHAPS) in the solubilization buffer; (2) extensive washing of the affinity resin with 10 mM CHAPS/0.06% asolectin/10% sucrose; and (3) elution with clorazepate, rather than flurazepam and urea. The binding of the $GABA_AR$ agonist [^{3}H]muscimol was assayed as described previously (Sawyer et al., 2002).

Photolabeling of purified $GABA_AR$. The peak [^{3}H]muscimol binding fraction (5 ml) from each affinity column elution was used for labeling without further dialysis or concentration. KCl was added to a final concentration of 0.1 M. An aliquot of $GABA_AR$ (~40 nM [^{3}H]muscimol binding sites; 2.5 ml for preparative labeling or 0.1–0.2 ml for analytical) was equilibrated with [^{3}H]azietomidate (final concentration, 1.5–3 μM) plus or minus additional drugs, incubated on ice for 1 h in the dark (4°C), and irradiated (30 min; 365 nm). After photolabeling, the total protein was precipitated with methanol/chloroform, solubilized in sample loading buffer, and fractionated by SDS-PAGE. The resulting gel lane was cut into 3 mm slices and eluted individually in 1 ml of elution buffer (Ziebell et al., 2004). The eluted bands were assayed for ^{3}H. Fractions of interest were filtered and concentrated, and the protein was precipitated with acetone and then resuspended in 50 μl of digestion buffer (25 mM Tris, pH 8.6, 0.1% SDS, 500 μM EDTA).

Enzymatic digestion, reversed-phase HPLC, and protein microsequencing. Digestion for 3 d at 25°C with the endoproteinases Lys-C (EndoLys-C) or Asp-N (EndoAsp-N) (Princeton Separations, Adelphia, NJ) was performed with 2.5 μg of protease in 10 μl of H_2O added to 50 μl of either labeled $GABA_AR$ in digestion buffer or, for EndoAsp-N, $GABA_AR$ diluted 10-fold with H_20 to reduce the SDS concentration to 0.01%. For V8 protease (ICN Biochemicals, Costa Mesa, CA), 100 μg in 50 μl was added to 50 μl of labeled $GABA_AR$. Reversed-phase HPLC and peptide microsequencing were performed as described previously (Ziebell et al., 2004). For sensitive detection of ^{3}H release, the Procise 492 protein Sequencer (Applied Biosystems, Foster City, CA) was modified such that five-sixth of each cycle was collected for counting and one-sixth was injected for phenylthiohydantoin (PTH)-amino acid analysis. For high sensitivity detection of PTH-amino acids, two-thirds of each cycle was injected for PTH-amino acid analysis, and only one-third was counted. PTH-amino acids were quantitated by peak heights over background, and the actual picomole quantities and counts per minute that were detected are plotted in the figures. To determine the amount of peptide sequenced, the individual residues were fit to the equation $I_x = I_0 \times R^x$, where I_x is the picomole quantity detected in cycle x, I_0 is the starting amount of the peptide, and R is the average repetitive yield. Treatment with *o*-phthalaldehyde (OPA) during sequencing was as described previously (Ziebell et al., 2004). OPA reacts preferentially with primary rather than secondary amines (i.e., proline) and can be used at any cycle of Edman degradation to block sequencing of peptides not containing an N-terminal proline (Brauer et al., 1984).

Molecular modeling. A homology model of a bovine $GABA_AR$ was constructed from the cryo-electron microscopy structure of the *Torpedo marmorata* nAChR [4 Å resolution; Protein Data Bank code 2BG9 (Unwin, 2005)] with the Insight II Molecular Modeling package (Accelrys, San Diego, CA). The helical paths of the nAChR structure were preserved. Alignments of the M1, M2, and M4 segments relied on conserved residues in those sequences (Ernst et al., 2005). The M3 alignment was poorly defined because there is no sequence conservation between the nAChR and $GABA_AR$ M3 segments. M3 was aligned in the nAChR structure to bring positions in α1M3 (Leu-300, Phe-303, and Ala-304) in proximity to α1Thr-267 (M2–12), consistent with cross-linking data (Jansen and Akabas, 2006). The resulting M2–M3 loop extended from α1Pro-278 to α1Val-283. Potential ligand binding pockets were identified by the program PASS (Brady and Stouten, 2000) with 1.8 Å diameter probes.

Results

Purification of brain $GABA_AR$ with retention of allosteric modulation by etomidate

To identify the amino acids photolabeled by [^{3}H]azietomidate, we developed protocols for $GABA_AR$ solubilization and purification that preserved the binding of etomidate/azietomidate and allowed the ~5000-fold purification required for isolation of $GABA_AR$ at a high degree of purity. Previous studies had identified conditions by using strong detergents (deoxycholate and Triton X-100) and harsh washing steps that allowed several thousand-fold purification (to 1500–3000 pmol [^{3}H]muscimol per milligram of protein) while preserving agonist and benzodiazepine binding, but these preparations had lost allosteric modulation of benzodiazepine binding by barbiturates and anesthetic agents (Sigel et al., 1983; Stauber et al., 1987). Allosteric modulation by barbiturates and etomidate are preserved by use of milder detergents such as CHAPS, but isolation of $GABA_AR$ at high purity and yield was problematic (Stephenson and Olsen, 1982; Sigel and Barnard, 1984; King et al., 1987). As an alternative purification strategy, we examined whether the use of the detergent $C_{12}E_9$, which was particularly effective for purification of serotonin 5-HT_3 receptors (Hovius et al., 1998), in conjunction with CHAPS would facilitate efficient purification of $GABA_AR$ with retention of allosteric modulation. We found that a combination of 4 mM $C_{12}E_9$ and 5 mM CHAPS was most efficient: it

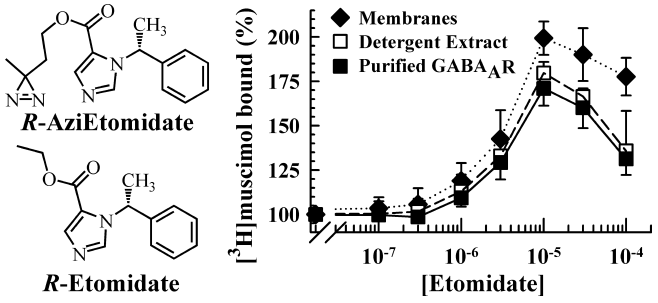

Figure 1. Etomidate modulation of [^{3}H]muscimol binding to bovine $GABA_AR$ in membrane suspensions (◆), detergent extracts (□), and after purification by affinity chromatography (■). Plotted are the percentage changes of specific [^{3}H]muscimol binding (5 nM) (mean ± SE) in the presence of increasing concentrations of etomidate. In each condition, the concentration for half-maximal potentiation was 3 ± 1 μM. The maximum potentiation seen at 10 μM etomidate did not differ significantly (one-way ANOVA; $p > 0.05$) for membrane-bound (199 ± 9%), detergent-solubilized (180 ± 6%), and purified $GABA_AR$ (171 ± 10%).

solubilized 60% of the [^{3}H]muscimol binding sites, in contrast to the 30% solubilization by 17 mM CHAPS. The etomidate modulation of [^{3}H]muscimol binding seen for membrane suspensions was preserved after solubilization and also after purification by affinity chromatography (Fig. 1). In each case, maximal potentiation was seen at 10 μM etomidate, with half-maximal potentiation at 3 μM, and etomidate at concentrations >10 μM produced a progressive decrease of [^{3}H]muscimol binding.

$GABA_ARs$ in the detergent extracts were purified at high yield and ~5000-fold by use of a benzodiazepine Ro7/1986–1 affinity column, extensive washing in the presence of 10 mM CHAPS/0.06% asolectin/10% sucrose, and elution with clorazepate. A representative purification (summarized in supplemental Table 1, available at www.jneurosci.org as supplemental material) resulted in 720 pmol of $GABA_AR$ (55% yield), which bound 3.4 nmol [^{3}H]muscimol per milligram of protein.

The purified $GABA_AR$ was characterized by SDS-PAGE with protein stain and immunoblot (Fig. 2). A single broad band centered at ~52 kDa was seen by Coomassie stain, but blots with subunit-specific antibodies revealed that the preparation consisted of a heterogeneous population of receptors. The peak of protein stain was closest to the molecular masses (kilodalton) of the antibodies specific for the α1(51), α2(53), β1(54), and β2(53) subunits, with the α3(59), α4(68), α5(57), and β3(56) subunits at lower mobility and γ2(47) at higher mobility. This observed $GABA_AR$ heterogeneity, which was also confirmed by liquid chromatography mass spectrometry/mass spectrometry analysis (supplemental Fig. 1, available at www.jneurosci.org as supplemental material), was expected, because the receptors were purified on a benzodiazepine affinity column that binds with high affinity all $GABA_ARs$ containing the γ2 subunit in combination with β subunits and α1, α2, α3, or α5 subunits (Sieghart, 1995).

[^{3}H]azietomidate photolabeling of $GABA_AR$

When purified $GABA_AR$ was photolabeled with 3 μM [^{3}H]azietomidate, all of the ^{3}H was recovered in the 50–58 kDa gel region, with the peak of ^{3}H at ~52 kDa, corresponding to the peak of Coomassie stain and the gel region enriched in α1, α2, and β1–3 subunits. GABA (1 mM) increased labeling by ~50% (Fig. 2*a*), and in the presence of GABA, etomidate produced a concentration-dependent inhibition of labeling characterized by an IC_{50} value of 30 μM, whereas the neurosteroid 3α,5α-tetrahydrodeoxycorticosterone (THDOC) (Wohlfarth et al., 2002) at 10 μM did not inhibit photolabeling (Fig. 3).

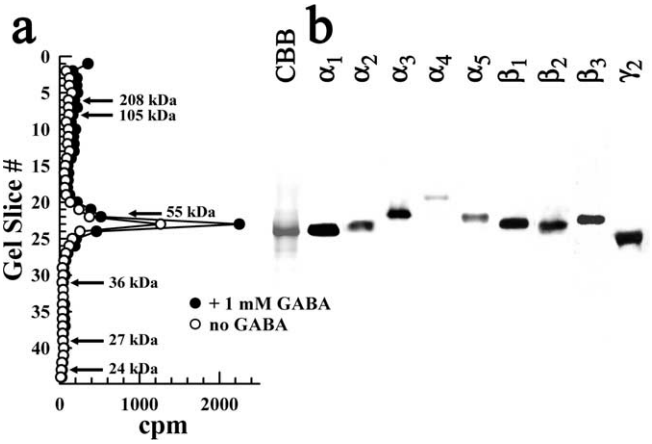

Figure 2. Photolabeling affinity-purified $GABA_AR$ with [^{3}H]azietomidate and characterization by immunoblot with subunit-specific antibodies. ***a***, $GABA_AR$ was labeled with 3 μM [^{3}H]azietomidate in the presence (●) or absence (○) of 1 mM GABA, and aliquots (15 pmol) were analyzed by SDS-PAGE, with the gel lanes cut into 3 mm slices to determine ^{3}H distribution by scintillation counting. The peak of ^{3}H, which was increased by 80% in the presence of GABA, had a mobility of 52 kDa that was similar to that of the Coomassie blue-stained band observed for a nonlabeled aliquot run on the gel in an adjacent lane (***b***, CBB). Also indicated are the relative positions of the molecular mass standards, which were shared by lanes in ***b***. ***b***, Coomassie stain and immunoblot characterization of aliquots of the same affinity column eluate fraction that was used for photolabeling. After electrophoretic transfer to polyvinylidene difluoride, strips were incubated with the indicated subunit-specific primary antibodies and then with secondary antibodies for visualization by chemiluminescence (see Materials and Methods). Shown are the results for a single experiment that was representative of results obtained with three different preparations of purified $GABA_AR$.

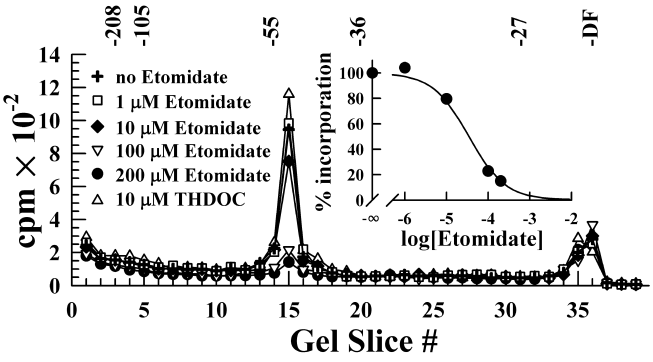

Figure 3. Etomidate inhibtion of $GABA_AR$ photolabeling. Etomidate produced a concentration-dependent inhibition of photolabeling (gel slice 15; IC_{50} value of 28 ± 4 μM; inset). The neurosteroid THDOC at 10 μM did not inhibit labeling.

To begin to identify the photolabeled amino acids, ^{3}H release profiles were determined by Edman degradation of proteolytic digests of the $GABA_AR$ subunits eluted from gel bands containing the peak of ^{3}H (~52 kDa) and from adjacent gel slices (~58 kDa). Proteolytic fragmentation was performed with Lys-specific EndoLys-C (Fig. 4*a*) or with the Glu-specific *Staphylococcus aureus* endopeptidase Glu-C (Fig. 4*b*, V8 protease). For both EndoLys-C digests, there were peaks of ^{3}H release in cycles 7 and 14, with the ^{3}H releases reduced by >90% for digests from $GABA_ARs$ labeled in the presence of 200 μM etomidate (data not shown). For the samples digested with V8 protease, there were peaks of ^{3}H release in cycles 16 and 27. The releases of ^{3}H in cycle 7 of the EndoLys-C digest and cycle 16 of the V8 digest were most prominent in the digests of the 58 kDa band, whereas the ^{3}H releases in cycles 14 of the EndoLys-C digest and 27 of the V8 digest were dominant in the digests of the 52 kDa band. These

results suggested that [^{3}H]azietomidate photolabeled subunits differentially enriched in the 52 and 58 kDa gel regions.

When EndoLys-C digests of each gel band were fractionated by reversed-phase HPLC, most of the ^{3}H eluted in a broad, hydrophobic peak (45–65% organic) (supplemental Fig. 2, available at www.jneurosci.org as supplemental material). For the 52 kDa band, protein microsequencing of fractions containing ^{3}H identified fragments beginning near the N termini of the αM1, αM3, and αM4 membrane-spanning segments, as well as some β subunit fragments (supplemental Fig. 1 and Table 2, available at www.jneurosci.org as supplemental material). For the 58 kDa band, fragments containing βM3 and βM4 were identified.

The protein microsequencing established that [^{3}H]azietomidate was incorporated into hydrophobic fragments, most likely one or several of the hydrophobic membrane spanning segments. Inspection of the location of potential EndoLys-C and V8 protease cleavage sites in terms of the subunit primary structures (Fig. 4*c*,*d*) revealed that the ^{3}H release profiles observed during radiosequence analyses were consistent with the labeling of the following: (1) α1Met-236 (and/or α2Met-235, α3Met-260, or α5Met-239), which is positioned in αM1 14 and 27 amino acids after α1Lys-222 and α1Glu-209, respectively; and (2) β1Met-286 (and/or β2Met-286 or β3Met-286), positioned in βM3, 7, and 16 amino acids after βLys-279 and βGlu-270, respectively. Because of the high degree of sequence conservation in these regions, including the protease cleavage sites, the predicted labeled amino acids could not be assigned to specific subunit subtypes, and therefore they will be referred to as αMet-236 (using the α1 subunit numbering) and βMet-286.

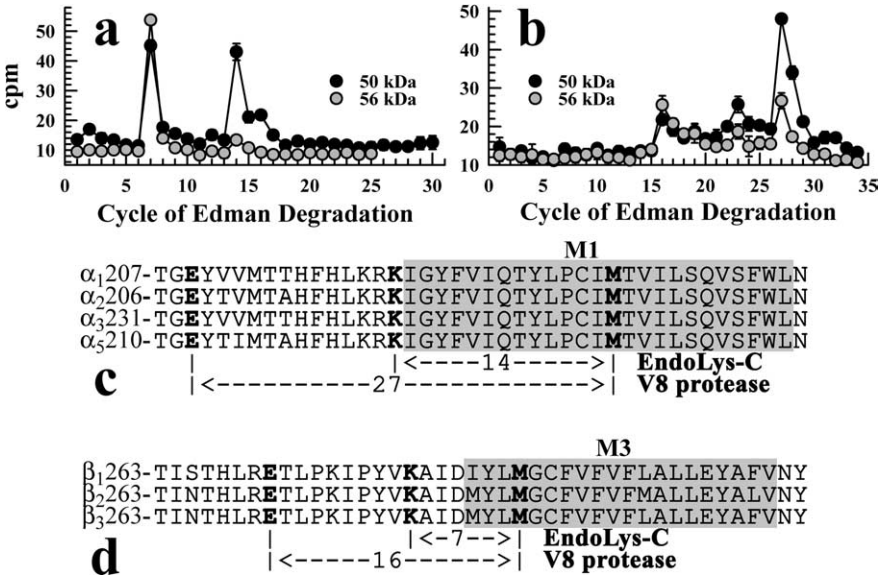

Figure 4. Edman sequencing of protease digests of [^{3}H]azietomidate-labeled $GABA_AR$ indicates α and β subunit labeling. ***a***, ***b***, ^{3}H release profiles observed after sequencing EndoLys-C (***a***) or V8 protease (***b***) digests of 52 kDa (black) or 58 kDa (gray) $GABA_AR$ subunits. Comparison of ^{3}H release profiles indicates that one labeled amino acid, detected primarily in the 52 kDa band, is 14/27 residues after a Lys/Glu, whereas the other is 7/16 residues after a Lys/Glu. ***c***, ***d***, Alignments of the bovine αM1 (***c***) and βM3 (***d***) sequences consistent with the ^{3}H release patterns illustrate homology between subtypes with conservation of labeling sites and protease sites (bold).

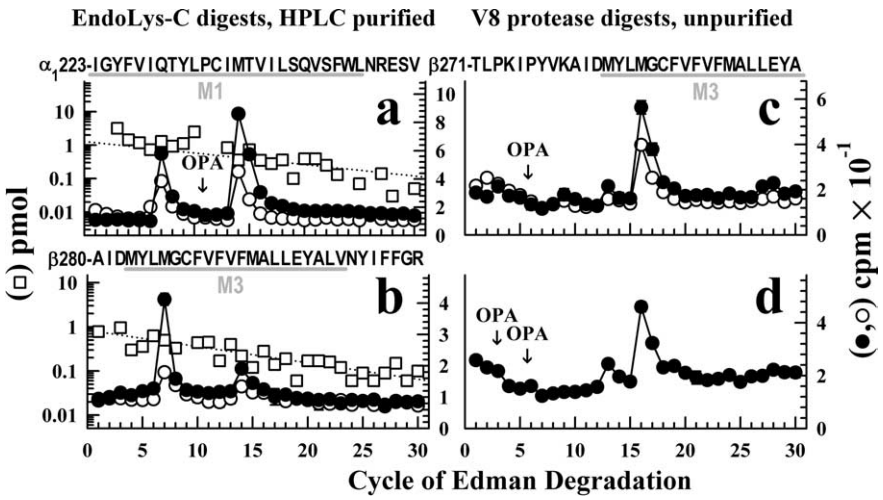

Figure 5. [^{3}H]azietomidate photolabels amino acids in αM1 (αMet-236) and βM3 (βMet-286). ***a-d***, ^{3}H release profiles (+GABA, ●; −GABA, ○), and picomoles of PTH-amino acid detected (+GABA only, □) during Edman sequencing. ***a***, Sequence analysis of the ^{3}H peak (3 fractions) from an HPLC purification (+GABA, 2430 cpm; −GABA, 1240 cpm) of an EndoLys-C digest of labeled $GABA_AR$ subunits (52–58 kDa) with OPA treatment in cycle 11. After OPA, sequencing persisted for the fragment beginning at αIle233, the N terminus of αM1 (+GABA □; I_0, 1.3 pmol, *R*, 92%; −GABA, I_0, 0.8 pmol, *R*, 95% (data not shown)]. Three additional sequences were present in the cycles before OPA: EndoLys-C Gly-1 (15 pmol), αIle-392 (αM4; 4 pmol), and αVal-280 (αM3; 3 pmol). Treatment with OPA reduced levels of those peptides by >90%. The persistence of ^{3}H release in cycle 14 indicated labeling of αMet-236 (330 cpm/pmol +GABA; 180 cpm/pmol −GABA). ***b***, Sequence analysis of the HPLC ^{3}H peak (+GABA, 580 cpm; −GABA, 320 cpm) from an EndoLys-C digest of labeled 58 kDa material identified fragments beginning at βAla-280 (□, +GABA, I_0, 0.8 pmol, *R*, 92%; −GABA, I_0, 0.5 pmol; *R*, 95%) as well as β3Ile-413 (βM4; 0.5 pmol) and EndoLys-C Gly 1 (1.8 pmol). The ^{3}H release in cycle 7 was consistent with labeling of βMet-286 (120 cpm/pmol +GABA; 50 cpm/pmol −GABA). ***c***, ***d***, ^{3}H release after sequencing V8 protease digests of labeled $GABA_AR$ subunits (52–58 kDa) without further purification. The βThr-271 sequence indicated above ***c*** is for reference but was not directly identified in these samples. Persistence of the ^{3}H release in cycle 16 after OPA treatment in cycle(s) 6 (***c***) or 3 and 6 (***d***) confirms [^{3}H]azietomidate labeling of βMet-286.

[^{3}H]azietomidate labels αMet-236 and βMet-286

Labeling of αMet-236 and βMet-286 was confirmed by taking advantage of the presence of prolines at positions preceding the predicted labeled amino acids and of an established sequencing protocol in which OPA, which reacts with primary amines, is applied before a cycle containing a proline to prevent Edman degradation of all peptides without an N-terminal proline (Brauer et al., 1984; Middleton and Cohen, 1991). When a sample from an HPLC purification of an EndoLys-C digest (Fig. 5*a*) was sequenced with OPA treatment at the predicted cycle for αPro-233, ^{3}H release was retained in cycle 14 (Fig. 5*a*), as expected for labeling of αMet-236, and the PTH-amino acids were present from the predicted fragment beginning at αIle-223. Labeling of αMet-236 was also confirmed by sequencing a V8 digest with OPA treatment at the cycle appropriate for αPro-233 (data not shown).

Sequence analysis of the ^{3}H peak from the HPLC purification of the EndoLys-C digest of the 58 kDa gel band identified a frag-

ment beginning at βAla-280 as the primary $GABA_AR$ subunit sequence, with release in cycle 7 consistent with GABA-enhanced labeling of βMet-286 (Fig. 5*b*). When samples from a V8 digest were sequenced with OPA treatment at the cycles predicted for βPro-273 and βPro-276, ^3H release was preserved in cycle 16, consistent with cleavage by V8 protease at βGlu-270 and labeling of βMet-286 (Fig. 5*c*,*d*).

The efficiencies of $GABA_AR$ photolabeling (counts per minute/picomole) at αMet-236 and βMet-286 were estimated from the ^3H releases at the appropriate cycles of Edman degradation and the amount of αM1 or βM3 fragment detected during sequence analysis of the HPLC purified fragments from EndoLys-C digests of the 52 and/or 58 kDa gel bands (Fig. 5*a*,*b*). The level of ^3H release in cycle 14 and the amount of the αM1 peptide indicated that αMet-236 was labeled at 330 (+GABA) and 180 cpm/pmol (−GABA) (Fig. 5*a*). Based on the levels of ^3H release in cycle 7 and the amount of the βAla-280 fragment in the samples (Fig. 5*b*), βMet-286 was labeled at 120 (+GABA) and 50 cpm/pmol (−GABA), i.e., at ~30% the efficiency of labeling of αMet-236. The combined efficiency of labeling at these two amino acids was close to the $GABA_AR$ photolabeling efficiency [770 and 410 cpm/pmol (±GABA)] estimated from the amount photolabeled (picomole quantities of [^3H]muscimol sites) and the total covalent ^3H incorporation measured after chloroform/methanol precipitation of the labeled $GABA_AR$. Based on the radiochemical specific activity of [^3H]azietomidate (11 Ci/mmol), for $GABA_ARs$ photolabeled with 3 μM [^3H]azietomidate in the presence of GABA, 3% of αMet-236 and 1% of βMet-286 were photolabeled. The efficiency of labeling will be determined both by the fractional site occupancy under our labeling conditions (~10%, based on the IC_{50} value of 30 μM for etomidate inhibition of photolabeling) and the intrinsic reactivities of the binding site side chains relative to the rate of reaction of the reactive species with the primary scavenger, water. Additional labeling studies at higher concentrations, as have been performed for [^3H]azietomidate labeling of the *Torpedo* nAChR (Ziebell et al., 2004), will be required to determine the efficiency of labeling at higher site occupancy.

Labeling of β2/3Asn-265?

Digestion of labeled $GABA_AR$ subunits with EndoLys-C or V8 protease cannot generate the cleavages necessary to identify labeling in βM2 at or near β2/3Asn-265, a major determinant of etomidate sensitivity *in vitro* (Belelli et al., 1997) and *in vivo* (Jurd et al., 2003; Reynolds et al., 2003), because there are no lysines or glutamates in the β subunit M1–M2 loop. The presence of an aspartate (β3Asp-243) in the M1–M2 loop of each β subunit, but not in the α subunits, indicated that digestion with EndoAsp-N could potentially reveal labeling in βM2, and we could also determine whether the enzyme could cleave effectively at βAsp-280 at the N terminus of M3, which would result in ^3H release from the labeled βMet-286 in the fifth cycle of Edman degradation. Sequence analyses of labeled subunits digested with EndoAsp-N resulted in no ^3H release above background either in cycle 5 or in the later cycles that would contain βM2 (β2/3Asn-265 would occur in cycle 21). The failure to observe ^3H release in cycle 5 indicated that under the conditions used, EndoAsp-N was not cleaving at βAsp-280, and there was also no evidence that it was cleaving in the M1–M2 loop. Additional studies are required to determine whether there is labeling in βM2 (or elsewhere in the $GABA_AR$); however, as noted above, the combined labeling efficiencies at αMet-236 and βMet-286 (450 cpm/pmol +GABA) were close to the total $GABA_AR$ labeling (770 cpm/pmol +GABA), so there cannot be another amino acid labeled at higher efficiency.

Discussion

In this work, we provide a first identification by use of photoaffinity labeling of amino acids contributing to a binding site for a general anesthetic in the $GABA_AR$, the *in vivo* target for the anesthetic action of etomidate. We used [^3H]azietomidate to photolabel $GABA_ARs$ purified from bovine cortex and then identified by protein microsequencing two labeled amino acids, one in an α subunit M1 membrane-spanning helix (αMet-236) and the other in a β subunit M3 membrane-spanning helix (βMet-286). Photoaffinity labeling provides an experimental approach to directly identify amino acids contributing to a drug binding site without determining whether the amino acid makes an important energetic contribution to drug binding. The photolabeled amino acid in βM3 was identified previously by mutational analyses as a sensitivity determinant for etomidate and propofol (Krasowski et al., 1998; Siegwart et al., 2002), and propofol protects against modification of a cysteine substituted at that position (Bali and Akabas, 2004). Our digestion strategies could not generate the cleavages in the M1–M2 loop necessary to identify photolabeling in βM2 at or near β2/3Asn265 (βM2–15), a major determinant of etomidate sensitivity *in vitro* (Belelli et al., 1997) and *in vivo* (Jurd et al., 2003; Reynolds et al., 2003); therefore, additional studies are required to determine whether labeling is there.

The binding of azietomidate and etomidate in proximity to an amino acid in the α subunit was not predicted by any previous work on etomidate or by the α subunit mutational analyses that identified sensitivity determinants for volatile anesthetics (Mihic et al., 1997; Krasowski et al., 1998; Nishikawa et al., 2002); however, the nature of the α subunit did affect the maximum etomidate potentiation of GABA responses or direct activation (Hill-Venning et al., 1997), and substitutions at the position in αM3 corresponding to βMet-286 decreased the EC_{50} values for activation by GABA, etomidate, or propofol (Krasowski et al., 1998).

Although the photolabeling results do not prove directly that αMet-236 and βMet-286 contribute to a common binding site, consideration of the experimental results in conjunction with homology models of the $GABA_AR$ TMD suggests strongly that azietomidate and etomidate both bind in proximity to the two labeled amino acids that are in a pocket at the interface between the β and α subunits. αMet-236 and βMet-286 were labeled at similar levels (330 and 120 cpm/pmol) and with similar pharmacological specificity; i.e., enhancement by GABA and inhibition by ~90% in the presence of 200 μM etomidate, consistent with the IC_{50} value of 30 μM seen for etomidate inhibition at the subunit level. In addition, azietomidate and other aliphatic diazirines preferentially label reactive side chains (Glu, Asp, and Tyr) in the nAChR and in soluble proteins (Pratt et al., 2000; Das et al., 2004; Ziebell et al., 2004). The lack of labeling of those side chains in αM1 (Tyr-225 and Tyr-231) and βM3 (Asp-282, Tyr-284, and Glu-298) provides evidence of the structural specificity of labeling and identifies regions in the TMD that do not contribute to the etomidate binding site.

An etomidate binding pocket in $GABA_AR$ homology models

We compared the location of the labeled amino acids in two $GABA_AR$ homology models, based on the *Torpedo* nAChR structure (Unwin, 2005), that differ subtly in the organization of the transmembrane α helices. The first model (Ernst et al., 2005) incorporates a two-amino-acid deletion in the M2–M3 loop of each $GABA_AR$ subunit resulting in a loop of four amino acids

beginning at α1Tyr-282. The second model, which is described in Materials and Methods, limits the M2–M3 loop to five amino acids extending from the conserved proline α1Pro-278 to α1Ala-283. In the nAChR structure and in both $GABA_AR$ models based on that structure, there are potential drug binding sites within aqueous pockets in the TMD that are within each subunit bundle of M1–M4 α-helices and are also at subunit interfaces bound by M1/M2 of one subunit and M2/M3 of an adjacent subunit. In the first model (data not shown), α_1Met-236 in αM1 is oriented toward the βM3 helix, suggesting an etomidate binding site at the interface of β and α subunits, but the labeled βMet-286 is oriented toward the interior of the β subunit transmembrane helical bundle. In this model, the two labeled amino acids contribute to two distinct pockets; however, α_1Met-236 is in close proximity to residues in βM3 (βGlu-298 and βTyr-299) that were not labeled but would have high intrinsic reactivity for the carbocation-reactive intermediate formed during irradiation of azietomidate. The lack of labeling of those reactive residues led us to develop a second homology model differing primarily in the disposition of amino acids in the M2–M3 loop and in M3.

In the homology model in Figure 6, the labeled amino acids (α1Met-236 and β3Met-286) are ~10 Å apart at the interface between the β and α subunits. Their side chains project toward a pocket, and this potential binding site for allosteric modulators in the TMD is at the same β–α interface as the binding pockets for GABA 50 Å above in the extracellular domain. Azietomidate can be accommodated readily in this pocket, as is shown in supplemental Figure 3 (available at www.jneurosci.org as supplemental material), which presents an expanded stereo view of the interface between the β and α subunits with the amino acids highlighted that project toward the pocket. Because βAsp-282 and βMet-283, which are positioned on the M3 helix one turn above βMet-286, are unlabeled, this suggests that βMet-286 defines the extracellular limit of the azietomidate binding site. The etomidate sensitivity determinant at βM2–15 (β1Ser-265/β2/3Asn-265) is at the level of αMet-236, which is accessible from both the intersubunit and intrasubunit pockets. The broad accessibility of βM2–15 predicted by this model may account for the fact that propofol does not protect from modification a cysteine substituted at this position, whereas it protects βM286C from modification (Bali and Akabas, 2004). Our model also predicts that αM2–15, a volatile anesthetic and alcohol sensitivity determinant (Mihic et al., 1997) and a position where propanethiol modification of a substituted cysteine results in persistent potentiation of GABA responses (Mascia et al., 2000), will be located equivalently to βM2–15 but at α–β and α–γ subunit interfaces.

A common binding site for agonist potentiation and direct gating

Etomidate and azietomidate, in common with most other general anesthetics, act at low concentrations to potentiate responses to submaximal GABA concentrations, with EC_{50} values of ~2 μM under usual assay conditions, and in the absence of GABA they directly activate the $GABA_AR$ with EC_{50} values of ~50 μM. Distinct sites for potentiation and direct activation have been proposed to account for the effects of substitutions at βM2–15 and at βMet-286 that differentially attenuate either potentiation by positive allosteric modulators or direct activation (Moody et al., 1997; Krasowski et al., 1998; Olsen et al., 2004); however, these varied phenomena can be accounted for by a mechanism in which etomidate binds to a common site resulting in potentiation or activation. GABA potentiation and direct activation share the same dependence on β subunit isoforms, the same stereoselectivity for etomidate (Tomlin et al., 1998) [and azietomidate (Husain et al., 2003)], and parallel responses for substitutions at βM2–15 (Belelli et al., 1997; Jurd et al., 2003). In addition, for wild-type $GABA_AR$, concentrations of etomidate up to 100 μM produce a progressive decrease of GABA EC_{50} values without evidence of saturation, and the data were well-fit by an allosteric model with each $GABA_AR$ containing two equivalent etomidate binding sites contributing to direct gating and agonist potentiation (Rusch et al., 2004). Thus, although the IC_{50} value of 30 μM for etomidate inhibition of $GABA_AR$ photolabeling is close to the EC_{50} value for direct gating, the experimental data presented here are consistent with the conclusion that αMet-236 as well as βMet-286 contribute to a single binding site responsible for potentiation and direct gating and that this binding site is located in the TMD at the interface between the β and α subunits.

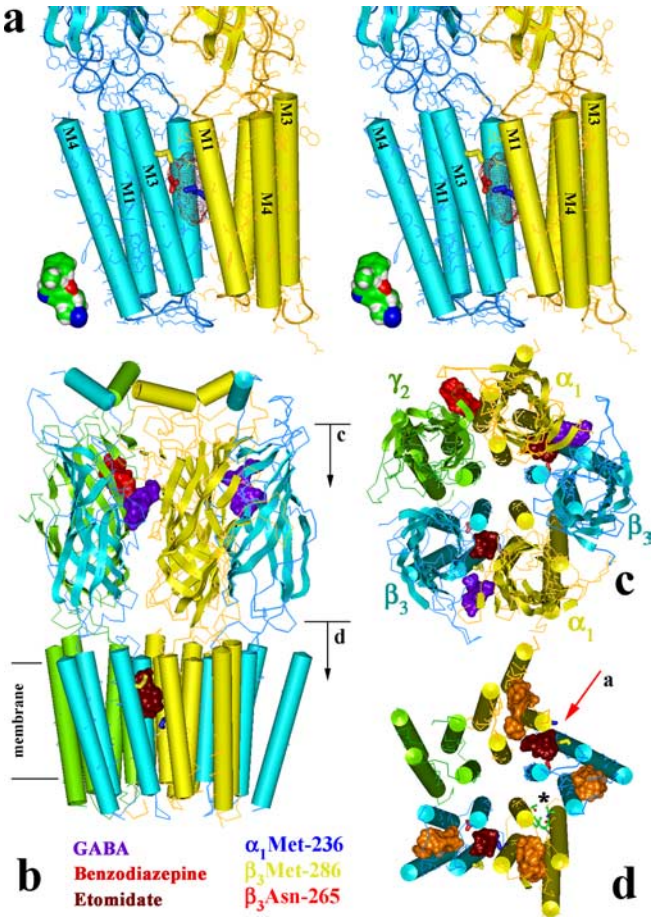

Figure 6. An azietomidate binding site in a $GABA_AR$ homology model. ***a***, Stereo image from within the membrane facing the interface of β3 (cyan) and α1 (yellow) subunits. A potential etomidate binding pocket at the subunit interface is shown as a dotted maroon Connolly surface with the labeled methionines (α1Met-236, blue; β3Met-286, yellow) and the etomidate affinity determinant β_3Asn-265 (red) (Belelli et al., 1997) projecting toward the pocket. Also shown is a Connolly surface representation of azietomidate. ***b–d***, Views of the $GABA_AR$ homology model (β_3, cyan; α_1, yellow; γ_2, green) from perspectives parallel to the membrane surface (***b***) or looking down the channel (***c***, ***d***) at levels indicated by the arrows in ***b***. Pockets in the vicinity of the binding sites for etomidate (maroon), GABA (purple), and benzodiazepine (red) are shown as Connolly surfaces. ***d***, Also included are potential intrahelical pockets in α_1 and β_3 (orange), the positions in α_1M2 and α_1M3 that as Cys mutants are susceptible to oxidative cross-linking (*) (Jansen and Akabas, 2006), and the perspective of ***a*** (red arrow).

References

Bali M, Akabas MH (2004) Defining the propofol binding site location on the $GABA_A$ receptor. Mol Pharmacol 65:68–76.

Belelli D, Lambert JJ, Peters JA, Wafford K, Whiting PJ (1997) The interaction of the general anesthetic etomidate with the gamma-aminobutyric acid type A receptor is influenced by a single amino acid. Proc Natl Acad Sci USA 94:11031–11036.

Brady GP, Stouten PFW (2000) Fast prediction and visualization of protein binding pockets with PASS. J Comp Mol Design 14:383–401.

Brauer AW, Oman CL, Margolies MN (1984) Use of *o*-phthalaldehyde to reduce background during automated Edman degradation. Anal Biochem 137:134–142.

Brejc K, van Dijk WJ, Klaassen R, Schuurmans M, van der Oost J, Smit AB, Sixma TK (2001) Crystal structure of AChBP reveals the ligand-binding domain of nicotinic receptors. Nature 411:269–276.

Corringer P-J, Le Novere N, Changeux J-P (2000) Nicotinic receptors at the amino acid level. Annu Rev Pharmacol Toxicol 40:431–458.

Cromer B, Morton CJ, Parker MW (2002) Anxiety over $GABA_A$ receptor structure relieved by AChBP. Trends Biochem Sci 27:280–287.

Das J, Addona GH, Sandberg WS, Husain SS, Stehle T, Miller KW (2004) Identification of a general anesthetic binding site in the diacylglycerol-binding domain of protein kinase C delta. J Biol Chem 279:37964–37972.

Duncalfe LL, Carpenter MR, Smillie LB, Martin IL, Dunn SMJ (1996) The major site of photoaffinity labeling of the γ-aminobutyric acid type A receptor by [^{3}H]flunitrazepam is histidine-102 of the α subunit. J Biol Chem 271:9209–9214.

Ernst M, Bruckner S, Boresch S, Sieghart W (2005) Comparative models of GABA(A) receptor extracellular and transmembrane domains: important insights in pharmacology and function. Mol Pharmacol 68:1291–1300.

Franks NP, Lieb WR (1994) Molecular and cellular mechanisms of general anaesthesia. Nature 367:607–614.

Hemmings HC, Akabas MH, Goldstein PA, Trudell JR, Orser BA, Harrison NL (2005) Emerging molecular mechanisms of general anesthetic action. Trends Pharmacol Sci 26:503–510.

Hill-Venning C, Belelli D, Peters JA, Lambert JJ (1997) Subunit-dependent interaction of the general anaesthetic etomidate with the γ-aminobutyric acid type A receptor. Br J Pharmacol 120:749–756.

Hovius R, Tairi A-P, Blasey H, Bernard A, Lundström K, Vogel H (1998) Characterization of a mouse serotonin $5\text{-}HT_3$ receptor purified from mammalian cells. J Neurochem 70:824–834.

Husain SS, Ziebell MR, Ruesch D, Hong F, Arevalo E, Kosterlitz JA, Olsen RW, Forman SA, Cohen JB, Miller KW (2003) 2-(3-Methyl-3*H*-diaziren-3-yl) ethyl 1-(1-phenylethyl)-1*H*-imidazole-5-carboxylate: a derivative of the stereoselective general anesthetic etomidate for photolabeling ligand-gated ion channels. J Med Chem 46:1257–1265.

Jansen M, Akabas MH (2006) State-dependent cross-linking of the M2 and M3 segments: functional basis for the alignment of $GABA_A$ and acetylcholine receptor M3 segments. J Neurosci 26:4492–4499.

Jurd R, Arras M, Lambert S, Drexler B, Siegwart R, Crestani F, Zaugg M, Vogt KE, Ledermann B, Antkowiak B, Rudolph U (2003) General anesthetic actions in vivo strongly attenuated by a point mutation in the GABA(A) receptor beta 3 subunit. FASEB J 17:250–252.

King RG, Nielsen M, Stauber GB, Olsen RW (1987) Convulsant/barbiturate activity on the soluble γ-aminobutyric acid–benzodiazepine receptor complex. Eur J Biochem 169:555–562.

Kotzyba-Hibert F, Kapfer I, Goeldner M (1995) Recent trends in photoaffinity labeling. Angew Chem Int Ed Engl 34:1296–1312.

Krasowski MD, Koltchine VV, Rick CE, Ye Q, Finn SE, Harrison NL (1998) Propofol and other intravenous anesthetics have sites of action on the γ-aminobutyric acid type A receptor distinct from that for isoflurane. Mol Pharmacol 53:530–538.

Mascia MP, Trudell JR, Harris RA (2000) Specific binding sites for alcohols and anesthetics on ligand-gated ion channels. Proc Natl Acad Sci USA 97:9305–9310.

Middleton RE, Cohen JB (1991) Mapping of the acetylcholine binding site of the nicotinic acetylcholine receptor: [^{3}H]-nicotine as an agonist photoaffinity label. Biochemistry 30:6987–6997.

Mihic SJ, Ye Q, Wick MJ, Koltchines VV, Krasowski MD, Finn SE, Mascia MP, Valenzuela CF, Hanson KK, Greenblatt EP, Harris RA, Harrison NL (1997) Sites of alcohol and volatile anaesthetic action on $GABA_A$ and glycine receptors. Nature 389:385–389.

Miyazawa A, Fujiyoshi Y, Unwin N (2003) Structure and gating mechanism of the acetylcholine receptor pore. Nature 423:949–958.

Moody EJ, Knauer C, Granja R, Strakhova M, Skolnick P (1997) Distinct loci mediate the direct and indirect actions of the anesthetic etomidate at $GABA_A$ receptors. J Neurochem 69:1310–1313.

Mourot A, Grutter T, Goeldner M, Kotzyba-Hibert F (2006) Dynamic structural investigations on the Torpedo nicotinic acetylcholine receptor by time-resolved photoaffinity labeling. Chembiochem 7:570–583.

Nishikawa K, Jenkins A, Paraskevakis I, Harrison NL (2002) Volatile anesthetic actions on the GABA(A) receptors: contrasting effects of alpha 1(S270) and beta 2(N265) point mutations. Neuropharmacology 42:337–345.

Olsen RW, Fischer JB, Dunwiddie TV (1986) Barbiturate enhancement of γ-aminobutyric acid receptor binding and function as a mechanism of anesthesia. In: Molecular and cellular mechanisms of anesthetics (Roth SH, Miller KW, eds), pp 165–177. New York: Plenum.

Olsen RW, Chang CSS, Li GD, Hanchar HJ, Wallner M (2004) Fishing for allosteric sites on GABA(A) receptors. Biochem Pharmacol 68:1675–1684.

Pratt MB, Husain SS, Miller KW, Cohen JB (2000) Identification of sites of incorporation in the nicotinic acetylcholine receptor of a photoactivatible general anesthetic. J Biol Chem 275:29441–29451.

Reynolds DS, Rosahl TW, Cirone J, O'Meara GF, Haythornthwaite A, Newman RJ, Myers J, Sur C, Howell O, Rutter AR, Atack J, Macaulay AJ, Hadingham KL, Hutson PH, Belelli D, Lambert JJ, Dawson GR, McKernan R, Whiting PJ, Wafford KA (2003) Sedation and anesthesia mediated by distinct $GABA_A$ receptor isoforms. J Neurosci 23:8608–8617.

Rusch D, Zhong HJ, Forman SA (2004) Gating allosterism at a single class of etomidate sites on alpha(1)beta(2)gamma(2L) GABA(A) receptors accounts for both direct activation and agonist modulation. J Biol Chem 279:20982–20992.

Sawyer GW, Chiara DC, Olsen RW, Cohen JB (2002) Identification of the bovine γ-aminobutyric acid type A receptor α subunit residues photolabeled by the imidazobenzodiazepine [^{3}H]Ro15–4513. J Biol Chem 277:50036–50045.

Sieghart W (1995) Structure and pharmacology of gamma-aminobutyric acid A receptor subtypes. Pharmacol Rev 47:181–234.

Siegwart R, Jurd R, Rudolph U (2002) Molecular determinants for the action of general anesthetics at recombinant alpha(2)beta(3)gamma(2) gamma-aminobutyric acid(A) receptors. J Neurochem 80:140–148.

Sigel E, Barnard EAA (1984) γ-Aminobutyric acid/benzodiazepine receptor complex from bovine cerebral cortex. J Biol Chem 259:7219–7223.

Sigel E, Stephenson FA, Mamalaki C, Barnard EA (1983) A γ-aminobutyric acid/benzodiazepine receptor complex of bovine cerebral cortex. J Biol Chem 258:6965–6971.

Sine SM, Engel AG (2006) Recent advances in Cys-loop receptor structure and function. Nature 440:448–455.

Smith GB, Olsen RW (1994) Identification of a [^{3}H]muscimol photoaffinity substrate in the bovine γ-aminobutyric acidA receptor α subunit. J Biol Chem 269:20380–20387.

Stauber GB, Ransom RW, Dilber AI, Olsen RW (1987) The γ-aminobutyric acid-benzodiazepine receptor protein from rat brain: large scale purification and preparation of antibodies. Eur J Biochem 167:125–133.

Stephenson FA, Olsen RW (1982) Solubilization by CHAPS detergent of barbiturate-enhanced benzodiazepine-GABA receptor complex. J Neurochem 39:1579–1586.

Tomlin SL, Jenkins A, Lieb WR, Franks NP (1998) Stereoselective effects of etomidate optical isomers on gamma-aminobutyric acid type A receptors and animals. Anesthesiology 88:708–717.

Unwin N (2005) Refined structure of the nicotinic acetylcholine receptor at 4 Á resolution. J Mol Biol 346:967–989.

Wohlfarth KM, Bianchi MT, MacDonald RL (2002) Enhanced neurosteroid potentiation of ternary $GABA_A$ receptors containing the δ subunit. J Neurosci 22:1541–1549.

Yamakura T, Bertaccini E, Trudell JR, Harris RA (2001) Anesthetics and ion channels: molecular models and sites of action. Annu Rev Pharmacol Toxicol 41:23–51.

Ziebell MR, Nirthanan S, Husain SS, Miller KW, Cohen JB (2004) Identification of binding sites in the nicotinic acetylcholine receptor for [^{3}H]azietomidate, a photoactivatable general anesthetic. J Biol Chem 279:17640–17649.